OPTIMAL FORCING FREQUENCY FOR ENHANCEMENT OF NEAR-WALL VORTICAL STRUCTURE IN A TURBULENT BOUNDARY LAYER

Kyoungyoun Kim
Department of Mechanical Engineering,
Korea Advanced Institute of Science and Technology,
373-1, Gusong-dong, Yusong-gu, Daejon, 305-701, KOREA
kyoungyoun@kaist.ac.kr

Hyung Jin Sung
Department of Mechanical Engineering,
Korea Advanced Institute of Science and Technology,
373-1, Gusong-dong, Yusong-gu, Daejon, 305-701, KOREA
hjsung@kaist.ac.kr

ABSTRACT

Effects of localized periodic blowing on a turbulent boundary layer are investigated using direct numerical simulation. The time-periodic blowing through a spanwise slot is given by varying the wall-normal velocity in a cyclic manner from 0 to $2A^+$. The time-periodic blowing frequency is given in a range $0 \leq f^+ \leq 0.08$ at a fixed blowing amplitude of $A^+=0.5$. Simulations of spatially-evolving turbulent boundary layer are carried out at the Reynolds numbers of 300 and 670 based on the momentum thickness and free-stream velocity. The effects of the blowing frequency are scrutinized by examining the phase- or time-averaged turbulent statistics. A most effective blowing frequency is obtained at $f^+=0.035$ for both Reynolds numbers, where the maximum increases of Reynolds shear stress, streamwise vorticity fluctuations and energy redistribution are made. Reynolds stress budget shows that the effective blowing frequency most enhances the pressure-strain term, which is closely related with the energy redistribution. The analysis of the phase-averaged stretching and tilting terms reveals that the stretching term is significantly enhanced in the 'downward' motion which is induced by the spanwise vortical motion.

INTRODUCTION

Advances in the understanding the coherent structure of wall-bounded turbulent flow have intensified interest in controlling the near-wall turbulence. Many attempts have been made to devise a practical method for controlling wall bounded flows. These include the modification of the wall surface by installing riblets (Choi et al., 1993), as well as the use of a compliant wall (Choi et al., 1997), a wall deformation (Kim et al., 2003) or a spanwise oscillating wall (Choi et al., 2002). Among the approaches considered to date, the use of local suction/blowing (Rebbeck and Choi, 2001; Jacobson and Reynolds, 1998) deserves more detailed study because it provides an efficient and simple means for locally actuating the wall-bounded flow. Moreover, the strength of the actuation can be controlled with relative ease by local suction/blowing. The local forcing in a turbulent boundary layer is also frequently encountered in many engineering applications. The local blowing is often used to protect the surface from high temperature in gas turbine or to cool the electronic chip.

Most previous experimental and numerical studies of local suction/blowing have focused on steady actuation (Sano and Hirayama, 1985; Park and Choi, 1999; Krogstad and Kourakine, 2000; Kim et al., 2002b). It is reported that the local steady blowing lifts up near-wall streamwise vortices, thereby reducing the interaction of the vortices with the wall. The steady blowing leads to a reduction in the skin friction near the wall, combined with an increase in the turbulent intensity and skin friction far downstream from the slot. In contrast to the previous studies that considered only steady blowing, a relatively few studies of unsteady suction/blowing were made experimentally and numerically (Park et al., 2001, 2003; Rhee and Sung, 2001; Tardu, 2001). Park et al. (2001) performed experiments to probe the effects of periodic blowing and suction through a spanwise slot on a turbulent boundary layer. Within their experimental condition, the higher forcing frequency induces greater changes in the turbulent structures of boundary layer. Tardu (2001) reported that with larger blowing frequency than a critical value ($f^+=0.008$), the blowing induces a positive wall vorticity layer which subsequently rolls up into a coherent spanwise vortex. However, since the above studies on the unsteady forcing employ a very large amplitude forcing (30∼40% of free-stream velocity) which changes the flow significantly, they focused on the evolution of a newly generated strong spanwise vortical structure due to the large amplitude forcing rather than on the response of the near-wall coherent structure. Recently, Kim and Sung (2003) investigated the effects of localized time-periodic blowing by carrying out direct numerical simulations for three cases of relatively small blowing amplitude (less than 5% of free-stream velocity). The energy redistribution is enhanced by the periodic blowing. Although it is expected that the turbulence structure is more sensitive to the blowing frequency than the blowing strength, they dealt with only a single blowing frequency ($f^+=0.017$).

It is known that near-wall streamwise vortices play a dominant role on wall bounded flow (Robinson 1990). However, the frequency responses of near-wall vortices to the unsteady periodic blowing were not studied in detail. In the present

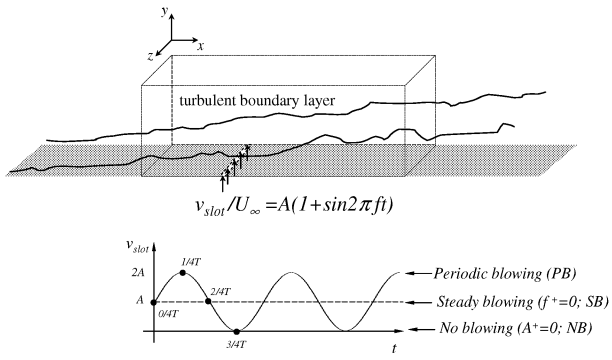

Figure 1: Schematic diagram of computational domain.

study, the effect of the blowing frequency on turbulent boundary layer is studied. Main emphasis of this study is placed on the blowing frequency effect on near-wall turbulent flow structures downstream of the spanwise slot. Direct numerical simulations are carried out for two Reynolds numbers $Re_{\theta,in}$=300 and 670 based on the momentum thickness and free-stream velocity. The slot width is approximately 100 in wall units and the localized time-periodic blowing is given by changing the wall-normal velocity on the spanwise slot. The blowing frequency is varied in a range of $0 \leq f^+ \leq 0.08$ at a fixed blowing amplitude (A^+=0.5). The frequency responses are scrutinized by examining the phase- or time-averaged turbulent statistics. A most effective blowing frequency is observed at f^+=0.035, where the maximum increases of Reynolds shear stress, streamwise vorticity fluctuations and energy redistribution are made. Reynolds stress budget analysis reveals that the effective blowing frequency most enhances the pressure-strain term. The phase-averaged stretching and tilting terms are analyzed to clarify the increase of streamwise vorticity fluctuations.

COMPUTATIONAL DETAILS

Direct numerical simulations of turbulent boundary layer for two Reynolds numbers Re_θ=300 and 670 are performed to probe the flow. The governing Navier-Stokes and continuity equations are integrated in time by using a fractional step method with an implicit velocity decoupling procedure (Kim et al., 2002a). A second-order central difference scheme is used in space with a staggered mesh. A schematic diagram of the computational domain is displayed in figure 1. The domain size and mesh resolution for the present DNS are summarized in table 1. Realistic velocity fluctuations at the inlet are obtained using the method of Lund et al. (1998). The convective out-flow condition $\frac{\partial u_i}{\partial t} + c\frac{\partial u_i}{\partial x} = 0$ is used at the exit, where c is taken to be the mean exit velocity. A no-slip boundary condition is imposed at the solid wall. At the free-stream, the conditions $u = U_\infty$ and $\frac{\partial v}{\partial y} = \frac{\partial w}{\partial y} = 0$ are imposed. Periodic boundary conditions are used in the spanwise direction. The streamwise width of spanwise slot for the localized blowing is $b^+ \approx 100$ in wall unit, which is comparable with that of Park and Choi (1999). The periodic blowing at the slot is generated by varying the wall-normal velocity according to the equation:

$$v_{slot}/U_\infty = A\,(1 + \sin 2\pi f t) \tag{1}$$

The blowing frequency ($f^+ = f\nu/u^2_{\tau,in}$) varies in a range $0 \leq f^+ \leq 0.08$, where $u_{\tau,in}$ is the friction velocity at the inlet.

Table 1: Domain size and mesh resolutions

Re_θ	(L_x,L_y,L_z)	(N_x,N_y,N_z)	Δx^+	Δz^+	Δy^+_{min}
300	(200,30,40)	(257,65,129)	12.3	4.92	0.17
670	(150,30,35)	(393,65,187)	12.6	5.88	0.20

Table 2: Localized blowing conditions

Re_θ	b/θ_{in}	b^+	A^+	$\overline{\sigma}$ $\left(\frac{Ab}{U_\infty \theta}\right)$	$\overline{\sigma}^+$ $\left(A^+ b^+\right)$	f^+ $\left(\frac{f\nu}{u^2_{\tau,in}}\right)$
300	6.25	99	0.5	0.14	50	0-0.08
670	3.06	101	0.5	0.064	50	0-0.08

Note that f^+=0 denotes the steady blowing ($v_{slot}/U_\infty = A$). Details regarding the localized blowing conditions are summarized in table 2. The imposition of periodic blowing may lead to periodic variations in the global physical quantities of the flow. Hence, it is necessary to represent each flow quantity as a superposition of three components

$$q(x,y,z,t) = \overline{q}(x,y) + \widetilde{q}(x,y,t) + q'(x,y,z,t) \tag{2}$$

where the instantaneous quantity q is decomposed into a time-mean component $\overline{q}$, an oscillating component $\widetilde{q}$ and a random fluctuating component q'. denotes The phase-averaged value is denoted as $\langle q \rangle = \overline{q} + \widetilde{q}$.

RESULTS AND DISCUSSION

To investigate the effects of periodic blowing on the near-wall turbulence, it is important to find the variations of streamwise vorticity fluctuations due to the periodic blowing. The relative increase of local maximum of streamwise vorticity fluctuations is defined as $\Delta\omega'_{x,max} = (\omega'_{x,max} - \omega'_{x,max,o})/\omega'_{x,max,o} \times 100$, where the subscript 'o' denotes 'no-blowing'. Figure 2 shows the relative increase of $\omega'_{x,max}$ versus the blowing frequency. The location of the local maximum ω'_x corresponds to the average location of the center of the streamwise vortices (Kim et al., 1987) As displayed in figure 2,

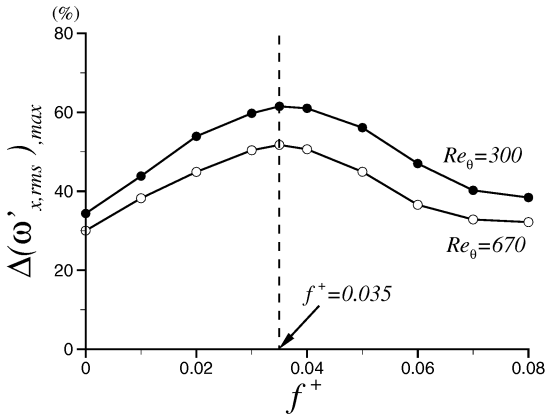

Figure 2: Relative increases of local maximum of $\omega_{x,max}$ due to the local blowing.

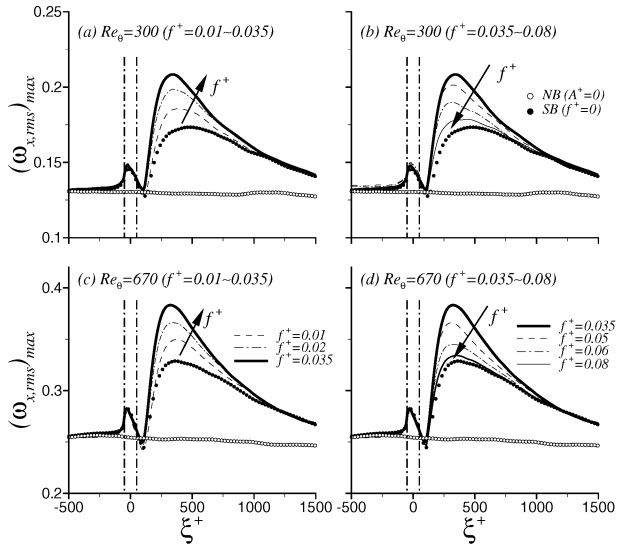

Figure 3: Variations of local maximum of ω'_x in the streamwise direction due to the periodic blowing.

$\omega'_{x,max}$ is significantly increased by the periodic blowing. The blowing frequency effect on the increase of $\omega'_{x,max}$ is clearly detected. It is obvious that $\Delta\omega'_{x,max}$ has a local maximum at f^+=0.035 for both Re=300 and 670. For Re=300, $\omega'_{x,max}$ is increased up to 60% by the periodic blowing (f^+=0.035) while 35% by the steady blowing, as compared with 'no-blowing'. This suggests the near-wall streamwise vortices are more enhanced by periodic blowing than by steady blowing and there exists an optimal blowing frequency (f^+=0.035 in the present study) for the activation of streamwise vortices by the localized blowing.

Figure 3 shows the variations of the local maximum values of streamwise vorticity fluctuations in the streamwise direction. The local maximum of ω'_x significantly increases at downstream due to the local blowing as compared with 'no-blowing' case. The blowing frequency effect of the evolution of $\omega'_{x,max}$ is clearly seen in the downstream. When f^+ is lower than the effective frequency (f^+=0.035), $\omega'_{x,max}$ at downstream becomes larger for both Re=300 and 670 as increases (figures 3a and 3c). However, when f^+ is higher than 0.035, $\omega'_{x,max}$ becomes smaller with increasing f^+ and converges to that of steady blowing (figures 3b and 3d). The unsteady effect of the periodic blowing on $\omega'_{x,max}$ is confined to the streamwise extent of ξ^+ ≈1000. It is clear that $\omega'_{x,max}$ is most increased at a particular blowing frequency (f^+=0.035) for both Re=300 and 670 as shown in figure 2. The maximum increase of $\omega'_{x,max}$ is shown at ξ^+ ≈=300

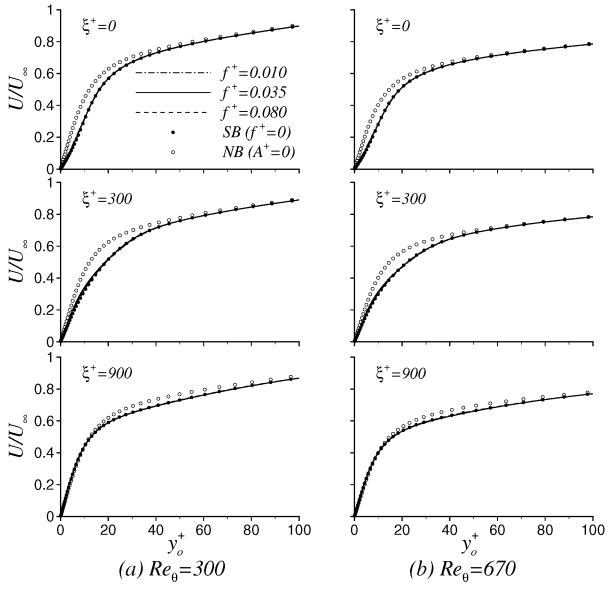

Figure 4: Time-averaged streamwise velocity profiles.

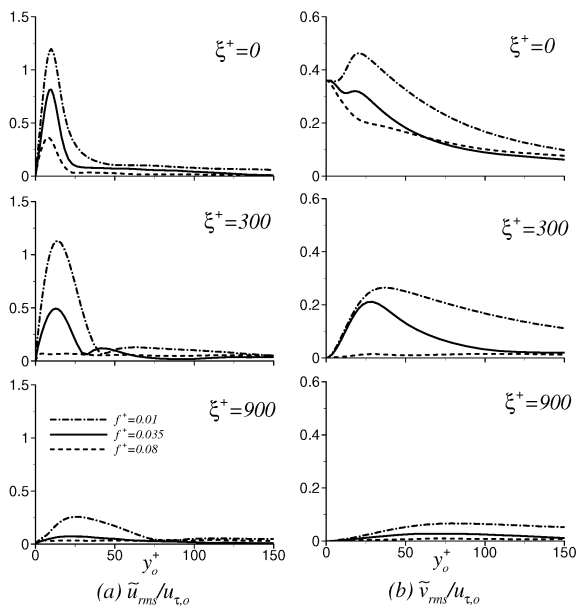

Figure 5: Oscillating component of phase-averaged velocity (Re=670).

Distributions of the time-averaged streamwise velocity at three locations (ξ^+=0, 300 and 900) are displayed in figure 4. Three cases of the blowing frequency are chosen for examining the variations of mean flow by unsteady blowing. The effective blowing frequency at f^+=0.035 gives the maximum increase of streamwise vorticity fluctuations. The lower and higher blowing frequencies are at f^+=0.01 and f^+=0.08, respectively. As compared to the case of 'no-blowing', a region of retarded flow is observed near the wall (ξ^+=0). As flow moves downstream, the region of retarded flow gradually shifts away from the wall and finally decays. However, the time-averaged streamwise velocity is invariant with the blowing frequency. This is consistent with the previous results (Tardu 2001).

Figure 5 shows the profiles of the rms of oscillating component of phase-averaged velocity for Re=670. The blowing frequency effect is clearly observed in contrast with the insensitivity of the mean-velocity to the unsteady blowing. As the blowing frequency increases, $\widetilde{u}_{rms}$ and $\widetilde{v}_{rms}$ decrease. At ξ^+=300, $\widetilde{u}_{rms}$ has double peaks whereas $\widetilde{v}_{rms}$ has a single peak. We also checked the phase of $\widetilde{u}$ and found that the double peaks of $\widetilde{u}_{rms}$ has a π phase difference, which indicates $\widetilde{u}$ has the opposite sign in the above and below the location of local minimum $\widetilde{u}_{rms}$. A closer inspection of $\widetilde{u}_{rms}$ at ξ=300 reveals that the second peak for f^+=0.035 is more distinct than those for other frequencies. It is also observed that location

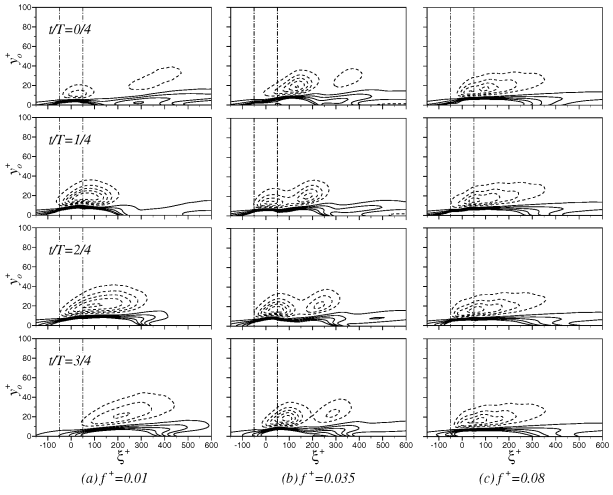

Figure 6: Contours of phase-averaged spanwise vorticity $\langle\omega_z\rangle$-$\overline{\omega}_{z,o}$ for Re=670. The contour levels are from -0.5 to 0.5 by increments of 0.1. The dashed lines denote the negative value.

of minimum $\widetilde{u}_{rms}$ for f^+=0.035 is closer to the wall as compared with that for f^+=0.01. The same results are observed in Re=300. The behaviors of $\widetilde{u}$ and $\widetilde{v}$ are consistent with the spanwise vortical motion in figure 6, where $\widetilde{u}$ undergoes the most intensive change with the opposite sign just above and below the center of the spanwise vortical motion. However, the maxima in $\widetilde{v}$ are located just upstream and downstream of the vortical motion at the same y location. The center of the spanwise vortical motion is located at the maximum $\widetilde{v}_{rms}$, which further shows a close agreement with the location of the local minimum of $\widetilde{u}_{rms}$ (Park et al., 2001).

Contours of the difference between the phase-averaged spanwise vorticity for periodic blowing $\langle\omega_z\rangle$ and the time-averaged spanwise vorticity for 'no-blowing' $\overline{\omega}_{z,o}$ in the case of Re=670 are shown in figure 6 during one period ($1T$). A negative region of $\Delta\langle\omega_z\rangle$, denoted by dashed line, appears above the slot for three cases. This is because a negative spanwise vorticity layer in the vicinity of the wall is shifted upward by blowing. Note that the negative (positive) value of $\Delta\langle\omega_z\rangle$ represents the increase (decrease) of the magnitude of spanwise vorticity since $\overline{\omega}_{z,o}$ is negative inside the boundary layer. For f^+=0.01, a region of strong negative vorticity is formed above the slot and moves convects as time goes by. During the accelerating phase (t=$0/4T$~$1/4T$), the formation of the strong negative vorticity occurs above the slot, which results from the lifted wall vorticity layer by blowing. The region of strong negative spanwise vorticity convects to downstream during the decelerating phase (t=$2/4T$~$3/4T$), when the adverse pressure gradient decreases above the slot. For f^+=0.035, a newly generated region of the strong spanwise vorticity coexists with the weaker prior one which convected in the decelerating phase of the previous period. For f^+=0.08, however, the phase difference is so small that the afore-stated unsteady responses, such as the convection of the negative $\Delta\langle\omega_z\rangle$, are not found.

Figure 7 shows the profiles of time-averaged turbulent intensities and Reynolds shear stress for Re=670 at ξ^+=300 where maximum increase of $\omega'_{x,max}$ occurs. The velocity fluctuations and Reynolds shear stress for blowing are increased as compared with the case of 'no-blowing'. It is interesting to

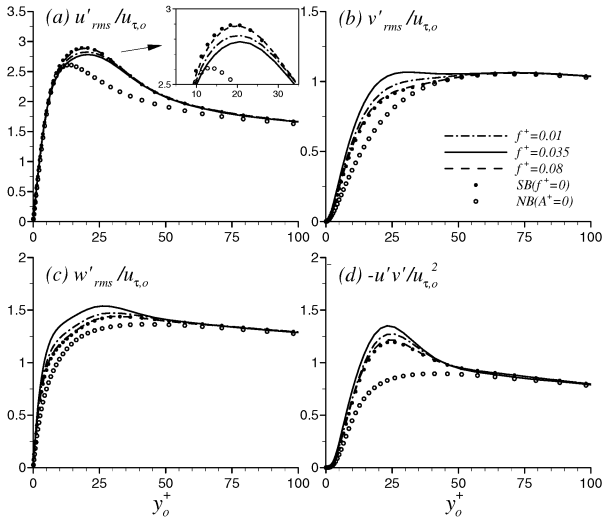

Figure 7: Time-averaged turbulent intensities and Reynolds shear stress at ξ^+=300 for Re=670.

find that the increase of u'_{rms} for f^+=0.035 is smaller than those for other frequencies, whereas the increase of v'_{rms}, w'_{rms} and $-\overline{u'v'}$ for f^+=0.035 are larger than those for other frequencies. This suggests that f^+=0.035 is the most effective blowing frequency in promoting the inter-component energy transfer between velocity fluctuations. The same conclusion is drawn for Re=300.

To investigate the inter-component energy transfer between the Reynolds-stress components, the time-averaged pressure-strain correlation terms $\phi_{ij} = \overline{p'(\frac{\partial u'_i}{\partial x_j} + \frac{\partial u'_j}{\partial x_i})}$ near the wall are represented in figure 8. It is known that the pressure-strain

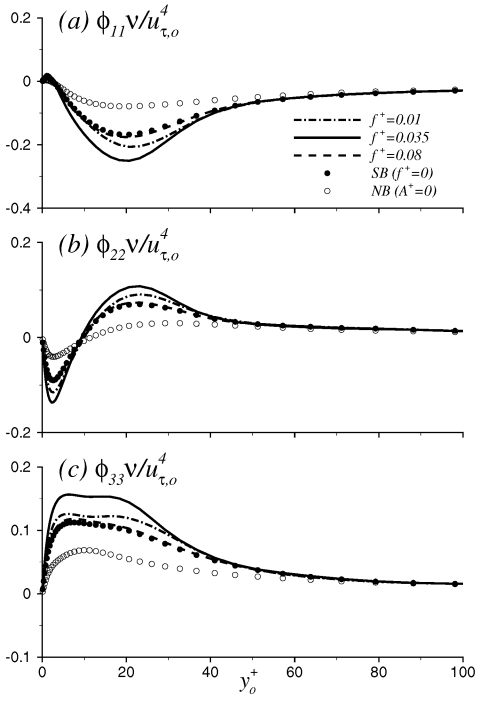

Figure 8: Pressure-strain correlation terms at ξ^+=300 for Re=670.

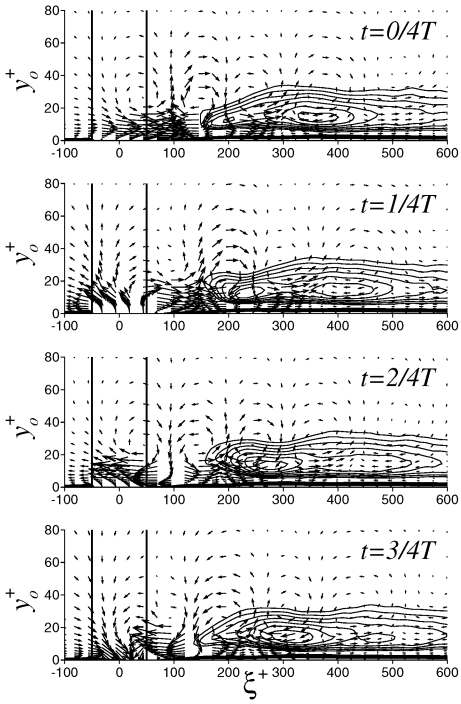

Figure 9: Contours of phase-averaged streamwise vorticity and vector plots of oscillating velocities for $f^+ = 0.035$ (Re=670).

term ϕ_{ij} plays a dominant role in the energy redistribution among the components. In the budget of turbulent kinetic energy, there is no net contribution from the pressure-strain term. Therefore, the negative sign of ϕ_{kk} (no summation on k) indicates a loss of energy from $u_k'^2$ or a transfer of energy from this component to other components, whereas the positive sign denotes an energy gain. ϕ_{ij} is significantly enhanced by the local blowing in the downstream, which is observed in turbulent channel flow with blowing (Chung and Sung, 2001) The present results exhibit that ϕ_{ij} is enhanced by the periodic blowing and is strongly dependent on the blowing frequency. The magnitudes of ϕ_{ij} is most increased by the effective blowing frequency f^+=0.035. Note that the enhancement of ϕ_{ij} for f^+=0.035 is nearly two times as large as those for the steady blowing, while ϕ_{ij} for f^+=0.08 is nearly the same as those of steady blowing. This indicates that the energy redistribution is most enhance at f^+=0.035, which is in agreement with the behaviors of turbulent intensities shown in figure 7. The same response of ϕ_{ij} on the blowing frequency is observed for Re=300. To examine the unsteady response of the streamwise vorticity fluctuations to the periodic blowing, a sequence of four snapshots showing the evolution of the phase-averaged streamwise vorticity fluctuations $\sqrt{\langle\omega_x'^2\rangle}$ is displayed in figure 9. The vector plots of the oscillating velocity components are superimposed to gain a better understanding of the flow evolution. The response of ω_x' is closely related to the oscillating velocity field. Behind the slot, a 'downward' motion is induced at ξ^+=200 in t/T=0/4, where ω_x' starts to increase and convects to the downstream. It is found that the 'downward' motion enhances the stretching term of the ω_x' transport equation (see below). On the other hand, an 'upward' motion is also induced by the blowing at ξ^+=300 in t/T=0/4. The 'upward' motion lifts the strengthened layer of due to

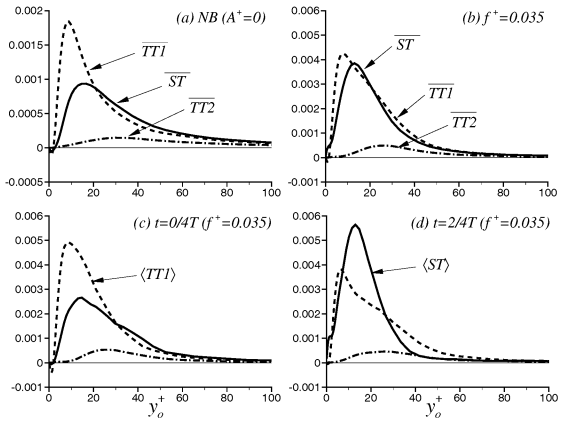

Figure 10: Stretching and tilting terms of streamwise vorticity transport equations at the location of ξ^+ =300 for Re=670. (a) Time-averages for NB, (b) Time-averages for $f^+ = 0.035$, (c) Phase-averages at $t = 0/4T$ for $f^+ = 0.035$, (d) Phase-averages at $t = 2/4T$ for $f^+ = 0.035$.

the 'downward' motion, thereby the interaction between the strengthened layer of ω_x' and the wall becomes weaker, and the lifted vortices get stronger. In the case of f^+=0.035, the streamwise wavelength of the 'downward' and 'upward' motions is approximately 200 in wall unit, which matches well with the streamwise length scale of near-wall vortical structures (Jeong et al. 1997). This suggests that one streamwise vortex undergoes both the 'downward' and 'upward' motions, which is responsible for the maximum increase of ω_x' at optimal blowing frequency (f^+=0.035). The dynamics equation for the strength of streamwise vorticity is written as

$$\frac{1}{2}\frac{D\omega_x}{Dt} = \underbrace{\omega_x^2\frac{\partial u}{\partial x}}_{ST} \underbrace{-\omega_x\frac{\partial w}{\partial x}\frac{\partial u}{\partial y}}_{TT1} \underbrace{+\omega_x\frac{\partial v}{\partial x}\frac{\partial u}{\partial z}}_{TT2} + \omega_x\frac{1}{Re}\nabla^2\omega_x \qquad (3)$$

Figure 10(a) shows the time-averaged value of stretching (ST) and tilting (TT1 and TT2) terms for 'no- blowing'. TT2 is negligible as compared with other terms (ST and TT1), which is consistent with the results of Brooke and Hanratty (1993). At y_o^+<10, the dominant term is tilting, while the stretching has nearly the same magnitude as the tilting for y_o^+>20. The same was observed in Park and Choi (1999). The time-averaged value of stretching and tilting terms at ξ^+=300 is shown in figure 10(b) for the periodic blowing (f^+=0.035). Note that the stretching and tilting terms for the periodic blowing is about 2 times larger than those for 'no-blowing' (figure 10a). The stretching term is significantly enhanced and is dominant even near the wall y_o^+<10, as compared with the case of 'no-blowing'. For the phase when the 'upward' and 'downward' motions take place at ξ^+=300, the phase-averaged stretching and tilting terms are represented in figures 10(c) and 10(d), respectively. At the phase of 'upward' motion, the stretching and tilting terms are increased as compared with that of 'no-blowing', however, the contribution of each term is nearly the same as that of 'no-blowing'. On the other hand, at the phase of 'downward' motion, the stretching term is so significantly increased that it is larger than tilting term TT1 at y_o^+=20. In the 'downward' motion, the streamwise vortices move closer to the wall and a negative $\widetilde{v}$ toward the wall leads that the flow spreads out near the wall, which enhances the

stretching term due to the increased $\partial u/\partial x$ >0 as the flow spreads out.

CONCLUSIONS

Detailed numerical analysis has been performed to see the effects of localized periodic blowing on a turbulent boundary layer. The time-periodic blowing through a span-wise slot is given by varying the wall-normal velocity in a cyclic manner from 0 to $2A^+$. The time-periodic blowing frequency is given in a range $0 \leq f^+ \leq 0.08$ at a fixed blowing amplitude of A^+=0.5. Direct numerical simulations of spatially-evolving turbulent boundary layer are carried out at the Reynolds numbers of 300 and 670 based on the momentum thickness and free-stream velocity. A most effective blowing frequency is observed at f^+=0.035, where the maximum increases of Reynolds shear stress, streamwise vorticity fluctuations and energy redistribution are made. The time-averaged streamwise velocity is invariant with the blowing frequency. However, the blowing frequency effect is clearly observed in the phase-averaged velocities. As the blowing frequency increases, $\widetilde{u}_{rms}$ and $\widetilde{v}_{rms}$ decrease. The velocity fluctuations and Reynolds shear stress for periodic blowing are increased as compared with the case of 'no-blowing'. The increase of u'_{rms} for f^+=0.035 is smaller than those for other frequencies, whereas the increase of v'_{rms}, w'_{rms} and $-\overline{u'v'}$ for f^+=0.035 are larger than those for other frequencies. This is consistent with the most enhancement of the pressure-strain term at the effective blowing frequency. The analysis of the phase-averaged streamwise vorticity and its stretching and tilting terms shows that the 'downward' motion of the phase-averaged velocity enhances the stretching term and the 'upward' motion lifts the strengthened layer of ω'_x, thereby the interaction between the strengthened layer of ω'_x and the wall becomes weaker, and the lifted vortices get stronger.

REFERENCES

Brooke, J. W., and Hanratty, T. H., 1993, "Origin of turbulence-producing eddies in a channel flow", *Physics of Fluids*, Vol. 5, pp. 1011-1022.

Choi, H., Moin, P., and Kim, J., 1993, "Direct numerical simulation of turbulent flow over riblets", *Journal of Fluid Mechanics*, Vol. 255, pp. 503-539.

Choi, J. -I., Xu, C. -X., and Sung, H. J., 2002, "Drag reduction by spanwise wall oscillations in wall-bounded turbulent flows", *AIAA Journal*, Vol. 40(5), pp. 842-850.

Choi, K. S., Yang, X., Clayton, B. R., Glover, E. J., Atlar, M., Semenov, B. N., and Kulik, V. M., 1997, "Turbulent drag reduction using compliant surfaces", *Proc. Royal Soc. London Series A*, Vol. 453, pp. 2229-2240.

Chung, Y. M., and Sung, H. J., 2001, "Initial relaxation of spatially evolving turbulent channel flow with blowing and suction", *AIAA Journal*, Vol. 39, pp. 2091-2099.

Jacobson, S. A., and Reynolds, W. C., 1998, "Active control of streamwise vortices and streaks in boundary layers", *Journal of Fluid Mechanics*, Vol. 360, pp. 179-211.

Jeong, J., Hussain, W., Schoppa, W., and Kim, J., 1997, "Coherent structures near the wall in a turbulent channel flow", *Journal of Fluid Mechanics*, Vol. 332, pp. 185-214.

Kim, C., Jeon, W. -P., Park, J., and Choi, H., 2003, "Effects of a localized time-periodic wall motion on a turbulent boundary layer flow", *Physics of Fluids*, Vol. 15(1), pp. 2142-2145.

Kim, J., Moin, P., and Moser, R., 1987, "Turbulence statistics in fully developed channel flow a low Reynolds number", *Journal of Fluid Mechanics*, Vol. 177, pp. 133-166.

Kim, K., Baek, S. -J., and Sung, H. J., 2002a, "An implicit velocity decoupling procedure for the incompressible Navier-Stokes equations", *International Journal for Numerical Method in Fluids*, Vol. 38(2), pp. 125-138.

Kim, K., and Sung, H. J., 2003, "Effects of periodic blowing from a spanwise slot on a turbulent boundary layer", *AIAA Journal*, Vol. 41(10), pp. 1916-1924.

Kim, K., Sung, H. J., and Chung, M. K., 2002b, "Assessment of local blowing and suction in a turbulent boundary layer", *AIAA Journal*, Vol. 40(1), pp. 175-177.

Krogstad, P. -Å., and Kourakine, A., 2000, "Some effects of localized injection on the turbulence structure in a boundary layer", *Physics of Fluids*, Vol. 12, pp. 2990-2999.

Lund, T. S., Wu, X., and Squires, K. D., 1998, "Generation of turbulent inflow data for spatially-developing boundary layer simulation", *Journal of Computational Physics*, Vol. 140, pp. 233-258.

Park, J., and Choi, H., 1999, "Effects of uniform blowing or suction from a spanwise slot on a turbulent boundary layer", *Physics of Fluids*, Vol. 11, pp. 3095-3105.

Park, S. -H., Lee, I., and Sung, H. J., 2001, "Effect of local forcing on a turbulent boundary layer", *Experiments in Fluids*, Vol. 31, pp. 384-393.

Park, Y. -S., Park, S. -H., and Sung, H. J., 2003, "Measurement of local forcing on a turbulent boundary layer using PIV", *Experiments in Fluids*, Vol. 34, pp. 697-707.

Rebbeck, H., and Choi, K. -S., 2001, "Opposition control of near-wall turbulence with a piston-type actuator", *Physics of Fluids*, Vol. 13, pp. 2142-2145.

Rhee, G. H., and Sung, H. J., 2001, "Numerical prediction of locally-forced turbulent boundary layer", *International Journal of Heat and Fluid Flow*, Vol. 22(6), pp. 624-632.

Robinson, S. K., 1991, "Coherent motions in the turbulent boundary layer", *Annual Reviews of Fluid Mechanics*, Vol. 23, pp. 601-639.

Sano, M., and Hirayama, N., 1985, "Turbulent boundary layer with injection and suction through a slit", *Bulletin of JSME*, Vol. 28, pp. 807-814.

Spalart, P. R., 1988, "Direct simulation of a turbulent boundary layer up to Re_θ=1410", *Journal of Fluid Mechanics*, Vol. 187, pp. 61-98.

Tardu, S. F., 2001, "Active control of near-wall turbulence by local oscillating blowing", *Journal of Fluid Mechanics*, Vol. 439, pp. 217-253.